

# A Near-Optimal Power Management Strategy for Rapid Component Sizing of Multimode Power Split Hybrid Vehicles

Xiaowu Zhang, Huei Peng, and Jing Sun, *Fellow, IEEE*

**Abstract**—In the design of hybrid vehicles, it is important to identify proper component sizes along with the optimal control. When the design search space is large, exhaustive optimal control strategies, such as dynamic programming (DP) is too time consuming to be used. Instead, a near-optimal method that is orders of magnitude faster than DP is needed. One such near-optimal method is developed and presented in this paper. This method is applied to identify the optimal powertrain parameters of all power-split hybrid configurations utilizing a single planetary gear. There are 12 possible configurations, six input and output splits, and each configuration has up to four modes. Based on the analysis of the efficiency of powertrain components of the four modes, and the power-weighted efficiency concept, we show that the computation time can be reduced by a factor of 10000 without consequential performance compromise, compared with the DP approach. The optimal design of each configuration is analyzed and presented.

**Index Terms**—Component sizing, energy management, hybrid vehicle, multiple modes, optimal control, optimal design, power-split.

## I. INTRODUCTION

THE market of hybrid vehicles has been dominated by power-split configuration for years—about 90% of the strong hybrid vehicles sold in the U.S. in 2012 are power-split type [1]. The configuration of a hybrid vehicle refers to the connection of powertrain components, [i.e., the engine, two motor/generators (MGs), and final drive] with the transmission, i.e., the three nodes of the planetary gear (PG). The popularity of the power-split hybrids can be attributed to their capability to take advantages of both series and parallel configurations [2], [3] and the high efficiency and compactness of the PG. Today's market leading power split designs, such as Toyota Prius, Ford Fusion, and Chevy Volt, all use a single PG as the transmission device. Some other models, such as Lexus GS450h and Toyota Highlander Hybrid, use two PGs that are simple extension of the single PG design. There are also hybrid designs that rely on PG systems in combat vehicles [3] and hybrid trucks [4].

Manuscript received December 4, 2013; accepted June 6, 2014. Date of publication July 31, 2014; date of current version February 11, 2015. Manuscript received in final form June 28, 2013. This work was supported by the Department of Energy under Award DE-PI0000012. Recommended by Associate Editor J. Lu.

X. Zhang and H. Peng are with the Department of Mechanical Engineering, University of Michigan, Ann Arbor, MI 48109 USA (e-mail: xiaowuz@umich.edu; hpeng@umich.edu).

J. Sun is with the Naval Architecture and Marine Engineering, University of Michigan, Ann Arbor, MI 48109 USA (e-mail: jingsun@umich.edu).

Color versions of one or more of the figures in this paper are available online at <http://ieeexplore.ieee.org>.

Digital Object Identifier 10.1109/TCST.2014.2335060

Using a single PG as the power split device can produce 12 possible configurations (six input and output splits) and each configuration can have up to four useful modes [5], whereas two PGs can produce 1152 combinations when two clutches are added [3]. While some of the configurations are protected by patents [6]–[8], there are many potential designs unexploited in this large candidate pool. The focus of this paper, however, is not to identify a particular configuration. Instead, we study a more fundamental problem: assuming all single-PG configurations are design candidates, how do we explore the full design space of configuration, namely the component sizing and control strategy design, to find the best hybrid vehicle design? When fuel economy is the main performance metric, sizing can be done through exhaustive search by finding an optimal energy management strategy for each of the sizing candidate. The control strategy can be solved using load leveling [9], [10], equivalent consumption minimization strategy (ECMS) [11], [12], the Pontryagin's minimum principle (PMP) [13]–[15], or dynamic programming (DP) [16], [17]. However, these strategies all have some limitations. Load leveling methods are not optimal, ECMS strategy is an instantaneous optimization method that requires tuning of the equivalent fuel consumption factor, DP incurs heavy computational load, and PMP frequently has numerical convergence issue for nonlinear two-point-boundary-value problems.

To mitigate these drawbacks, a rapid power management algorithm with the drive cycle information used in a statistical way is proposed and presented. DP, as the only approach that guarantees global optimality, will be used as the benchmark to verify the optimality of the proposed method.

This paper is organized as follows. In Section II, we illustrate the dynamics of the power-split system, including its mode operations. In Section III, the rapid near-optimal power management algorithm is described and a comparison among DP, ECMS, and the proposed algorithm is presented. In Section IV, two case studies to design the best input-split hybrid vehicle and the best output-split hybrid vehicle are presented with discussion on the optimal designs made and the benefit of having multiple clutches elaborated. Finally in Section V, the conclusion is stated.

## II. DYNAMICS OF POWER-SPLIT POWERTRAIN

### A. Dynamics of PG System

A PG system consists of a ring gear, a sun gear, and a carrier with several pinion gears. Its schematic together with a lever

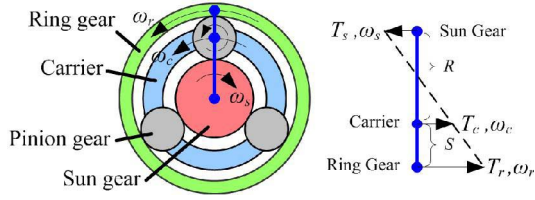


Fig. 1. Planetary gear and its lever analogy.

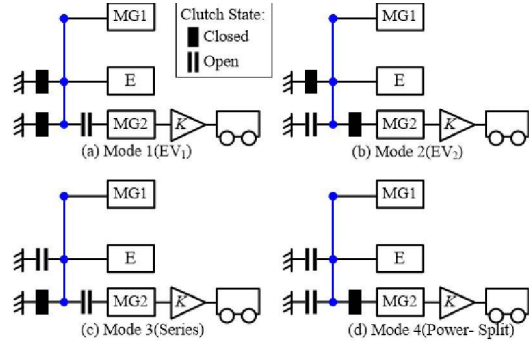


Fig. 2. All feasible modes for input-split configurations.

analogy is demonstrated in Fig. 1. A PG has two degrees of freedom (DoF), and the rotational speeds and acceleration of the three nodes (sun gear, ring gear, carrier) must follow the constraint

$$\omega_s S + \omega_r R = \omega_c (R + S) \quad (1)$$

where  $T_{(\cdot)}$  and  $\omega_{(\cdot)}$  denote the torque and speed, the subscript  $s$ ,  $r$ , and  $c$  indicate the sun gear, the ring gear, and the carrier, respectively.  $S$  and  $R$  are the radii of the sun gear and ring gear.

The dynamics of a single PG can be represented by (2), where  $I_{(\cdot)}$  is the inertia of the components connected to the nodes and  $F$  is the internal force between gear teeth

$$\begin{bmatrix} I_s & 0 & 0 & -S \\ 0 & I_r & 0 & -R \\ 0 & 0 & I_c & S+R \\ -S & -R & S+R & 0 \end{bmatrix} \begin{bmatrix} \dot{\omega}_s \\ \dot{\omega}_r \\ \dot{\omega}_c \\ F \end{bmatrix} = \begin{bmatrix} T_s \\ T_r \\ T_c \\ 0 \end{bmatrix} \quad (2)$$

### B. Multiple-Mode Operation

In [5], it was shown that when the engine is not directly connected to the output shaft and the two MGs are not collocated, there are twelve possible configurations: six input-split configurations (when one MG is connected to the output shaft) and six output-split configurations (when one MG is connected to the engine). For any given configuration, clutches can be added to enable different operation modes. It is shown that at most four feasible modes can be achieved when three clutches are added [5]. The modes for input-split configurations are shown in Fig. 2 and for the output split are shown in Fig. 3, where EV stands for Electric Vehicle drive mode.

Using rules stated in [19], the input split's dynamic equations can be obtained, which are shown in (3)–(6). The dynamics for output-split configurations are shown from (7)–(10).

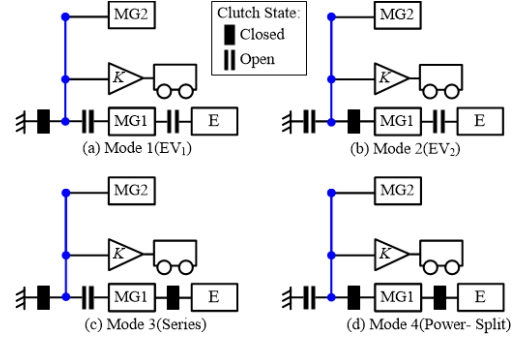


Fig. 3. All feasible modes for output-split configurations.

#### Input Split:

##### Mode 1 (EV<sub>1</sub>)

$$\left( \frac{mr^2}{K^2} + I_{MG2} \right) \dot{\omega}_{out} = T_{MG2} - T_{Load}. \quad (3)$$

##### Mode 2 (EV<sub>2</sub>)

$$\begin{bmatrix} I_e & 0 & 0 & 0 \\ 0 & \frac{mr^2}{K^2} + I_{MG2} & 0 & D_2 \\ 0 & 0 & I_{MG1} & D_3 \\ 0 & D_2 & D_3 & 0 \end{bmatrix} \begin{bmatrix} \dot{\omega}_e \\ \dot{\omega}_{out} \\ \dot{\omega}_{MG1} \\ F \end{bmatrix} = \begin{bmatrix} 0 \\ T_{MG2} - T_{Load} \\ T_{MG1} \\ 0 \end{bmatrix} \quad (4)$$

##### Mode 3 (Series)

$$\begin{bmatrix} I_e & 0 & 0 & D_1 \\ 0 & \frac{mr^2}{K^2} + I_{MG2} & 0 & 0 \\ 0 & 0 & I_{MG1} & D_3 \\ D_1 & 0 & D_3 & 0 \end{bmatrix} \begin{bmatrix} \dot{\omega}_e \\ \dot{\omega}_{out} \\ \dot{\omega}_{MG1} \\ F \end{bmatrix} = \begin{bmatrix} T_e \\ T_{MG2} - T_{Load} \\ T_{MG1} \\ 0 \end{bmatrix} \quad (5)$$

##### Mode 4 (Power Split)

$$\begin{bmatrix} I_e & 0 & 0 & D_1 \\ 0 & \frac{mr^2}{K^2} + I_{MG2} & 0 & D_2 \\ 0 & 0 & I_{MG1} & D_3 \\ D_1 & D_2 & D_3 & 0 \end{bmatrix} \begin{bmatrix} \dot{\omega}_e \\ \dot{\omega}_{out} \\ \dot{\omega}_{MG1} \\ F \end{bmatrix} = \begin{bmatrix} T_e \\ T_{MG2} - T_{Load} \\ T_{MG1} \\ 0 \end{bmatrix} \quad (6)$$

#### Output Split:

##### Mode 1 (EV<sub>1</sub>)

$$\begin{bmatrix} I_{MG1} + I_e & 0 & 0 & 0 \\ 0 & \frac{mr^2}{K^2} & 0 & D_2 \\ 0 & 0 & I_{MG2} & D_3 \\ 0 & D_2 & D_3 & 0 \end{bmatrix} \begin{bmatrix} \dot{\omega}_{MG1} \\ \dot{\omega}_{out} \\ \dot{\omega}_{MG2} \\ F \end{bmatrix} = \begin{bmatrix} 0 \\ -T_{Load} \\ T_{MG2} \\ 0 \end{bmatrix} \quad (7)$$

*Mode 2 (EV<sub>2</sub>)*

$$\begin{bmatrix} I_{MG1} & 0 & 0 & D_1 \\ 0 & \frac{mr^2}{K^2} & 0 & D_2 \\ 0 & 0 & I_{MG2} & D_3 \\ D_1 & D_2 & D_3 & 0 \end{bmatrix} \begin{bmatrix} \dot{\omega}_{MG1} \\ \dot{\omega}_{out} \\ \dot{\omega}_{MG2} \\ F \end{bmatrix} = \begin{bmatrix} T_{MG1} \\ -T_{Load} \\ T_{MG2} \\ 0 \end{bmatrix} \quad (8)$$

*Mode 3 (Series)*

$$\begin{bmatrix} I_{MG1} + I_e & 0 & 0 & 0 \\ 0 & \frac{mr^2}{K^2} & 0 & D_2 \\ 0 & 0 & I_{MG2} & D_3 \\ 0 & D_2 & D_3 & 0 \end{bmatrix} \begin{bmatrix} \dot{\omega}_{MG1} \\ \dot{\omega}_{out} \\ \dot{\omega}_{MG2} \\ F \end{bmatrix} = \begin{bmatrix} T_{MG1} + T_e \\ -T_{Load} \\ T_{MG2} \\ 0 \end{bmatrix} \quad (9)$$

*Mode 4 (Power Split)*

$$\begin{bmatrix} I_{MG1} + I_e & 0 & 0 & D_1 \\ 0 & \frac{mr^2}{K^2} & 0 & D_2 \\ 0 & 0 & I_{MG2} & D_3 \\ D_1 & D_2 & D_3 & 0 \end{bmatrix} \begin{bmatrix} \dot{\omega}_{MG1} \\ \dot{\omega}_{out} \\ \dot{\omega}_{MG2} \\ F \end{bmatrix} = \begin{bmatrix} T_{MG1} + T_e \\ -T_{Load} \\ T_{MG2} \\ 0 \end{bmatrix} \quad (10)$$

where elements  $D_1$ ,  $D_2$ , and  $D_3$  are permutations of  $-R$ ,  $-S$ , and  $R+S$ , they denote the configuration of the hybrid system. More specifically,  $-R$  is used if the powertrain component is connected to the ring gear,  $-S$  is used if the powertrain component is connected to the sun gear, and  $R+S$  is used if the powertrain component is connected to the carrier.  $\dot{\omega}_{out}$  is the angular acceleration of the output node.  $T_{Load}$  is defined in (11), where  $K$  is the final drive ratio,  $T_{fb}$  is the braking torque,  $R_{tire}$  is the radius of the tire,  $f_r$  is the coefficient of the rolling friction,  $\rho$  is the air density,  $A$  is the frontal area, and  $C_d$  is the air drag coefficient

$$T_{Load} = \frac{1}{K} \left[ T_{fb} + mgf_r R_{tire} + 0.5\rho AC_d \left( \frac{\omega_{out}}{K} \right)^2 R_{tire}^3 \right] \quad (11)$$

For the first three feasible modes of input-split configurations, the dynamics are trivial since Modes 1 and 2 have only 1 DoF while Mode 3 is a series mode; similar trivial dynamics can be found in the first and third mode of the output-split configurations. However, some assumptions must be made to analyze the split mode for both configurations and EV<sub>2</sub> mode for output-split configuration before we can proceed with the fast sizing approach.

*C. Split-Mode Analysis*

Since the power-split mode has 2 DoF, we can denote  $\alpha$  as the ratio between  $\dot{\omega}_e$  and  $\dot{\omega}_{out}$ . The system behavior can then be described by  $\alpha$  and  $\dot{\omega}_{out}$ . The acceleration lever diagram is shown in Fig. 4, which presents some possible acceleration combinations for input-split configurations [18].

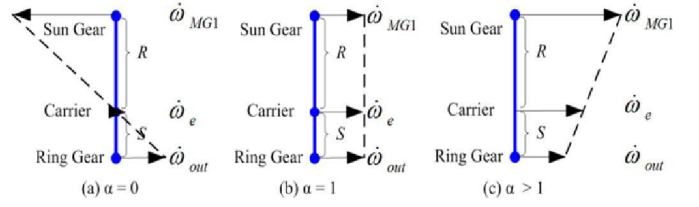


Fig. 4. Different acceleration cases in the power-split mode.

From (6), equation for MGs' torque calculation can be obtained as

$$\begin{bmatrix} T_{MG1} \\ T_{MG2} \end{bmatrix} = \begin{bmatrix} -\left[ (I_e \frac{D_3}{D_1} + I_{MG1} \frac{D_1}{D_3})\alpha + I_{MG1} \frac{D_2}{D_3} \right] \dot{\omega}_{out} + T_e \frac{D_2}{D_1} \\ T_{Load} + T_e \frac{D_2}{D_1} - \left( I_e \frac{D_2}{D_1} \alpha - \left( \frac{mr^2}{K^2} + I_{MG2} \right) \right) \dot{\omega}_{out} \end{bmatrix} \quad (12)$$

Specifically, when applying Prius' vehicle parameters, (12) becomes

$$\begin{bmatrix} T_{MG1} \\ T_{MG2} \end{bmatrix} = \begin{bmatrix} (0.14\alpha - 0.068)\dot{\omega}_{out} - 0.28T_e \\ T_{Load} - 0.72T_e - (0.13\alpha - 6.7)\dot{\omega}_{out} \end{bmatrix} \quad (13)$$

From (12) or (13),  $T_{MG1}$  and  $T_{MG2}$  can be solved if  $\dot{\omega}_{out}$ ,  $\alpha$ ,  $T_e$ , and  $T_{load}$  are given. A large  $\alpha$  will quickly lead to engine or MG1 speed saturation and unsmooth powertrain operation. Therefore, the value of  $\alpha$  should be kept close to unity in normal operations. It can be seen that the MGs' torque will not be affected much with an  $\alpha$  within the practical range, since the inertia of other powertrain components are much smaller than the inertia of the vehicle. Similar analysis can be applied to the EV<sub>2</sub> mode for output split configurations, and again the relative acceleration ratio between the MG and the output shaft does not have significant influence on the torque distribution.

To enable fast sizing and vehicle acceleration test in the split-mode, the acceleration ratio  $\alpha$  is assumed to be close to one (i.e., all components accelerate with the output shaft at the same rate) to reduce 1 DoF. This simplification was found to result in good performance compared with DP [19]. During the vehicle 0–60 mi/h acceleration test, the battery power limit is assumed to be 100 kW. In the following, when the drivability constraint is imposed, we require the vehicle to have a 0–60 mi/h time of 10 s or less to be considered drivable.

### III. POWER-WEIGHTED EFFICIENCY ANALYSIS FOR RAPID SIZING

In general, energy loss minimization could be a very effective way to optimize control strategy for EV mode, it will lead to no engine operation in hybrid mode. ECMS, a well-known instantaneous optimization method, could be applied to compare EV and hybrid modes. However, since the strategy is not inherently designed for multiple-mode hybrid vehicles and does not utilize the overall cycle information, the mode shift timing could not be decided sensibly. Moreover, it requires a recursive calculation to determine the equivalent fuel consumption factor for each sizing candidate, leading to

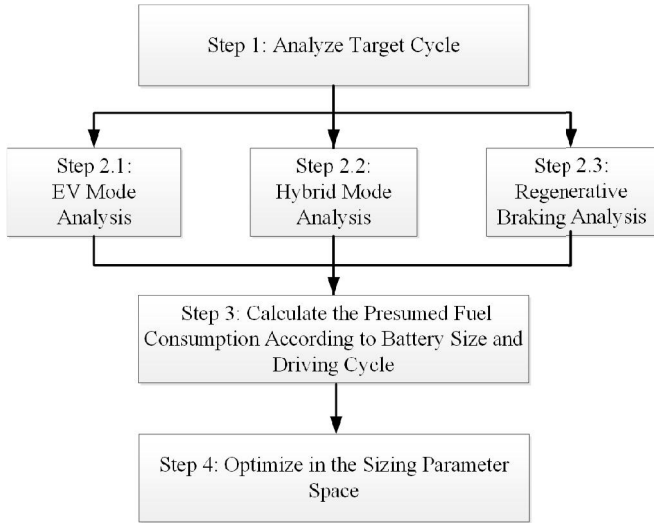


Fig. 5. Flowchart of PEARS.

a heuristic trial-and-error procedure. Whereas the proposed method, named as power-weighted efficiency analysis for rapid sizing (PEARS), can systematically address arbitrary desired battery energy consumption. Meanwhile, the control sequence and operation status for PEARS are based on optimal efficiency analysis with no heuristic trial-and-error required. Therefore, we choose PEARS instead of ECMS to design multimode plug-in hybrid vehicles.

In this section, we will first describe the procedure of PEARS. Subsequently, a comparison study is done among ECMS, PEARS, and DP.

### A. Procedure of PEARS

The PEARS concept proposed in this paper is based on efficiency analysis of powertrain components. For a given drive cycle, we consider all possible vehicle speeds and load combinations and rearrange them into a 2-D table. By looping through all possible components' speed and torque in each cell of that table, referred as vehicle speed-acceleration cell (SAC) in the following context, we can find the best efficiency and best power-weighted efficiency (PE) for given vehicle operation.<sup>1</sup> The battery open circuit voltage and internal resistance are assumed to be constant. The process of PEARS is summarized in Fig. 5 and detailed as follows.

*Step 1:* The speed and acceleration data for a target cycle are extracted. As an example, Fig. 6 shows the speed and acceleration profiles of Federal Urban Driving Schedule (FUDS) cycle. Data of the target cycle are collected and arranged into a 2-D matrix, as shown in Fig. 7.

*Step 2:* In Step 2, the EV modes, hybrid modes, and the regenerative braking case are analyzed separately. The best efficiencies, PEs, and their control argument will be recorded. The controls for PEARS are shown in Table I

<sup>1</sup>Noise, vibration and harshness (NVH) consequence caused by mode shift will not be considered in this analysis. However, it should be considered in the design of the mode switch control algorithm.

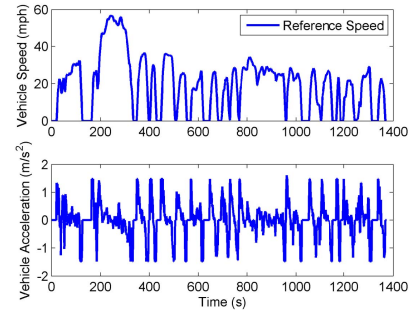


Fig. 6. Speed and acceleration profile of FUDS cycle.

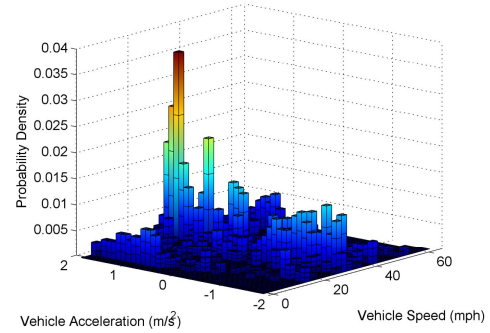


Fig. 7. Probability density of FUDS cycle.

TABLE I  
CONTROLS FOR EACH MODE IN PEARS

Configurations	Mode1	Mode2	Mode3	Mode4
Input-split	$T_{MG2}$	$T_{MG1}$	$T_e, \omega_e$	$T_e, \omega_e$
Output-split	$T_{MG2}$	$\omega_{MG1}$	$T_e, \omega_e$	$T_e, \omega_e$

and detailed description of efficiency calculation follows from Steps 2.1 to 2.3.

*Step 2.1:* The efficiency of the EV modes is defined in (14), where  $P_{EV}^{loss}$  is the loss of the EV mode being analyzed, including battery loss and electric-mechanical loss,  $P_{EV}^{in}$  refers to the power flows into the system. In the driving case,  $P_{EV}^{in}$  is the battery power. For modes with 1 DoF and use more than one MG, all possible torque combinations will be compared and the best PE will be recorded. For the EV mode with 2 DoF, according to the analysis in Section II-C, the accelerations of all powertrain components are assumed to be the same. All possible speed combinations for the EV 2-DoF mode will be considered. The best possible efficiency for each mode will be calculated according to (15), where  $\eta_{EV}^*$  corresponds to the optimal efficiency in each mode at certain vehicle speed and acceleration ( $\omega_{out}, \dot{\omega}_{out}$ ). The mode with superior efficiency will be considered as the EV mode for each SAC

$$\eta_{EM} = 1 - \frac{P_{EM}^{loss}}{P_{EM}^{in}} \quad (14)$$

$$\eta_{EV}^*|_{\omega_{out}, \dot{\omega}_{out}} = \max[\eta_{EV}(T_{MG1}, T_{MG2})]|_{\omega_{out}, \dot{\omega}_{out}} \quad (15)$$

*Step 2.2:* For each vehicle SAC, as defined in Section II, there are two hybrid modes: power-split mode and series mode. For the power-split mode, the vehicle load torque is calculated

TABLE II  
POWER FLOW OF THE HYBRID SYSTEM

Power flow	Description
$P_{e_1}$	Engine power which goes through the generator to the battery
$P_{e_2}$	Engine power which goes through generator to motor
$P_{e_3}$	Engine power which directly flows to the final drive
$P_{batt}$	Battery power when it is positive; 0 when the battery power is negative

from (11). By assuming  $\alpha = 1$ , the torque of MG1 and MG2 can be solved by looping through all possible engine torques using (12). For the series mode, the torque of MG1 is chosen to balance the engine torque while the torque of MG2 is calculated to satisfy the vehicle driving demand.

There are two possible power sources for the hybrid mode: the engine and the battery. In general, the power used by the system can be divided into four parts, as shown in (Table II, where  $P_{e_1} + P_{e_2} + P_{e_3}$  is equal to the total engine output power.  $P_{batt}$  is the battery power consumed. The PE is calculated in (16), where  $P_{fuel}$  stands for the fuel power; footnotes  $G$  and  $M$  stand for generator (when the power is negative) and motor (when the power is positive or zero); and  $\eta_{e\_max}$ ,  $\eta_{G\_max}$ , and  $\eta_{M\_max}$  are the highest efficiency of the engine, generator, and the motor. Due to the fact that the engine efficiency is much lower than the efficiency of the electrical system, the engine operation will not be selected if normalization is not applied

$$\eta_{Hybrid}(\omega_e, T_e) = \frac{P_{e_1}\eta_G\eta_{batt}/(\eta_{e\_max}\eta_{G\_max})}{P_{fuel} + P_{batt}} + \frac{P_{e_2}\eta_G\eta_M/(\eta_{e\_max}\eta_{G\_max}\eta_{M\_max})}{P_{fuel} + P_{batt}} + \frac{P_{e_3}/\eta_{e\_max} + P_{batt}\eta_{batt}\eta_M/\eta_{M\_max}}{P_{fuel} + P_{batt}} \quad (16)$$

$$\eta_{Hybrid}^* \Big|_{\omega_{out}, \dot{\omega}_{out}} = \max[\eta_{Hybrid}(\omega_e^*, T_e^*)] \Big|_{\omega_{out}, \dot{\omega}_{out}} \quad (17)$$

Fig. 8 describes the power-flow paths where  $\mu$  indicates whether the battery assist is ON. Note that in the series mode,  $P_{e_3} = 0$ .

*Step 2.3:* When the vehicle decelerates, regenerative braking is applied and the EV mode with the best efficiency is chosen following the process explained in Step 2.1. The calculation of PE follows (14) and (15), with  $P_{EV}^{in}$  defined as the mechanical power into the system.

*Step 3:* Once the best PE for both EV and hybrid modes are calculated for each SAC, for the next step, we will determine whether the vehicle should operate in the hybrid or EV mode for each SAC. Then, the presumed fuel consumption (PFC) can be calculated. The flowchart of Step 3 is shown in Fig. 9 and detailed calculation involved is described as follows.

*Step 3.1:* Given the battery size, the total available battery energy  $E_{av}$  is calculated. For example, in this paper, the available battery energy is assumed to be 0.9 kWh to enable both EV and hybrid operations. This amount of battery energy

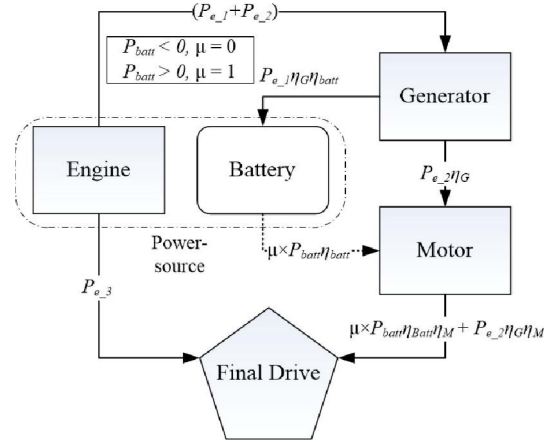


Fig. 8. Power flow of the hybrid mode.

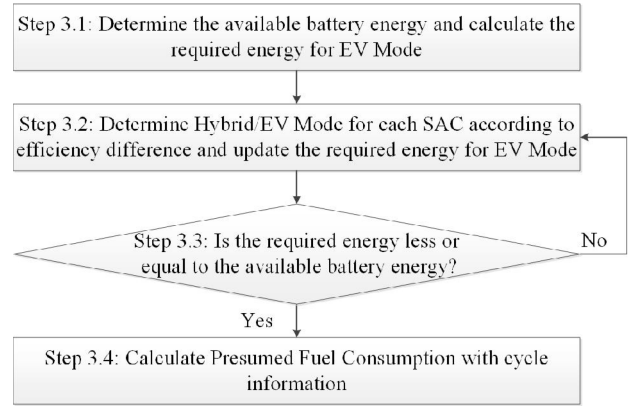


Fig. 9. Flowchart of Step 3.

is enough for close to 3 mi of driving, which is fairly significant for the urban cycle of  $\sim 7$ -mi long.

We first assume all the SACs operate in the EV modes, and the total required energy  $E_{EV}$  is calculated using (18), where  $N$  and  $M$  are the total number of SAC in driving and braking operation, respectively.  $\Phi_k$  and  $\Phi_l$  are the probability density of the  $k$ th and  $l$ th SAC,  $T_D$  and  $T_B$  are the total time durations,  $P_k^{EV}$  and  $P_l^{EV}$  are the battery power with optimal efficiency  $\eta_{EV}^*$  in the  $k$ th and  $l$ th SAC in the EV mode

$$E_{EV} = \sum_{k=1}^N P_k^{EV} \Phi_k T_D + \sum_{l=1}^M P_l^{EV} \Phi_l T_B \quad (18)$$

*Step 3.2:* The PE difference  $\eta_{Hybrid}^* - \eta_{EV}^*$  is calculated for each SAC in driving condition. The SAC with highest difference is chosen (assuming it is the  $j$ th SAC) for hybrid operation and the required energy  $E_{EV}$  will be updated based on (19), where  $P_j^{Hybrid}$  is the battery power in the hybrid mode

$$E_{EV\_new} = E_{EV} + P_j^{Hybrid} \Phi_j T_D - P_j^{EV} \Phi_j T_D \quad (19)$$

*Step 3.3:* Step 3.2 is repeated until  $E_{EV}$  is less than or equal to  $E_{av}$ . If after looping through all SAC and  $E_{EV}$  is greater than  $E_{av}$ , the battery power will be limited below zero in hybrid mode and the optimization will be run for one more time. If the  $E_{EV}$  is still greater than  $E_{av}$  after the battery power constraint, it indicates that the current sizing design candidate

TABLE III  
COMPARISON BETWEEN THREE ENERGY MANAGEMENT  
STRATEGIES FOR FUDS/HWFET CYCLE

Energy management strategy	Fuel (g)	Difference with DP	Computation time
DP	108.3/297.5	N/A	13h/7h
PEARS	114.2 /323.2	5.5%/8.6%	5.2s/2.9s
ECMS	118.0/323.3	9.0%/8.6%	$n \times (25.9s/15.0s)$

TABLE IV  
COMPARISON BETWEEN DP AND PEARS IN MODE  
OPERATION IN THE FUDS CYCLE

Energy management strategy	Fuel (g)	Percentage			
		Mode1	Mode2	Mode3	Mode4
DP	94.1	0%	89.66%	0%	10.34%
PEARS	100.5	1.75%	91.55%	0%	6.70 %

is not capable of finishing the cycle and it will be marked as an infeasible design.

*Step 3.4:* After determining the SACs that will be operated in the hybrid mode, the PFC is calculated from (20), where  $n_H$  is the number of SAC using the hybrid mode

$$PFC = \sum_{i=1}^{n_H} \text{fuel}_i \Phi_i T_D \quad (20)$$

*Step 4:* Steps 2 and 3 are repeated for each sizing design candidate, until all sizing parameters are looped through. The design with the lowest PFC is recorded as the optimal achievable for the corresponding candidate.

#### B. Comparison Study Among PEARS, ECMS, and DP

To study the performance of the proposed PEARS algorithm, we fix the vehicle design to be the same as Prius 2010 vehicle, with its key parameters shown in Table V.

The fuel consumption and computation time of the three control strategies are shown in Table III, where  $n$  (usually 4–5) in the ECMS row indicates the number of iterations to find the correct fuel equivalent factor to achieve the desired final State Of Charge (SOC). For PEARS, the final SOC can be arbitrarily specified and no iteration is needed. Therefore, PEARS is more suitable for Plug-in Hybrid Electric Vehicle (PHEV) optimal design studies compared with the ECMS strategy. Both ECMS and PEARS are about four orders of magnitude faster than DP.

Since ECMS was not originally designed for multiple-mode hybrid vehicles, the comparison study of multiple-mode operation is established only between PEARS and DP. As shown in Table IV, the difference in fuel economy between PEARS and DP is about 6% and both methods share similar mode occupation.

In summary, the PEARS strategy produces results close to those of DP, and the computation time is much shorter. While the ECMS strategy is also fast, it is not inherently designed for PHEV design, and not for multimode operations.

TABLE V  
DESIGN VARIABLES

Parameters	Configurations		Design variation range
	<i>Input-Split (Prius plug-in)</i>	<i>Output-Split (Volt 2012)</i>	
<i>Engine</i>	98 hp @5200rpm, 105 lbft @4000rpm	83 hp @4800rpm, 93 lbft @4800rpm	Fixed
<i>Vehicle mass(kg)</i>	1450	1750	Fixed
<i>FR</i>	3.2	2.16	2:0.5:5
<i>R:S</i>	2.6	2.24	1.6:0.2:3
$P_{MG1max}$	42kW Max speed 10000 rpm	54kW Max speed 6000 rpm	Can be down sized to 50% of the original size
$P_{MG2max}$	60kW Max speed 13500 rpm	111kW Max speed 9500 rpm	Can be down sized to 50% of the original size

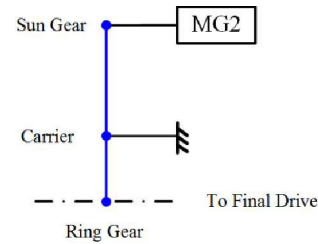


Fig. 10. Fixed gear ratio between MG2 and the final drive for input-split configuration.

Therefore, the PEARS method will be used for the sizing study for the remainder of this paper.

#### IV. DESIGN OF POWER-SPLIT HYBRID VEHICLES

In this section, the PEARS method is applied to all six input-split and six output-split configurations of single-PG hybrid vehicles with four operating modes to identify their best designs. For each configuration, four design variables are explored and their ranges of variation are shown in Table V. The optimal design results are compared with the Prius plug-in and Chevy Volt for input- and output-split configurations, respectively, as described in Table V. Note that there is a speed reduction of 2.63 between MG2 and the final drive for all six input-split configurations, the same as the design of Prius, which is shown in Fig. 10. This speed reduction ratio can be treated as another design variable, but for simplicity, it is not explored in this paper.

To exam the effectiveness of PEARS in the rapid sizing study, the Prius' and Volt's parameters are used as initial design values for all six input-split and six output-split configurations. All four design variables are allowed to vary. Both input- and output-split configurations are allowed to use all four modes mentioned in Section II.

The PEARS introduced in Section III is applied to all 12 configurations. The calculation time for each configuration on the FUDS cycle with PEARS is around 3 h on a server

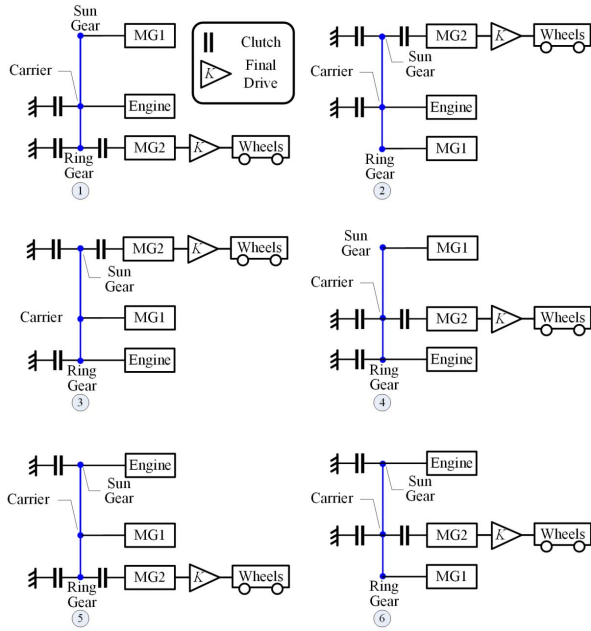


Fig. 11. Six input-split configurations using a single planetary gear.

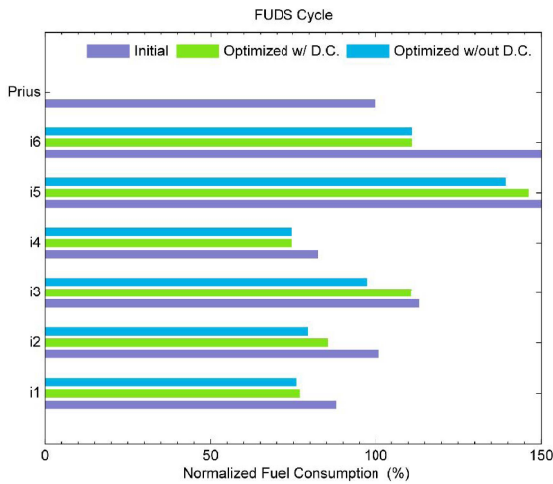


Fig. 12. Normalized fuel consumption results of the initial design and optimized design for the input split on the FUDS cycle.

with Xeon 2.8 GHz and 16-G RAM, compared with about 3.5 years it would take if DP had been used.

*A. Input-Split Configurations*

All six input-split configurations and three series of data are shown in Figs. 11 and 12, where D.C. stands for drivability constraint that requires the vehicle to be able to accelerate from 0 to 60 mi/h within 10 s. It is obvious that without drivability constraint, better fuel economy can be achieved. On the other hand, it should be also noted that even under the drivability constraint, the proposed rapid sizing method leads to significant fuel economy improvement for all configurations.

The optimized parameters for the drivable designs, its corresponding normalized fuel consumptions and the normalized fuel consumptions of the initial benchmarks are shown

TABLE VI  
OPTIMIZED DESIGN PARAMETERS AND FUEL CONSUMPTION FOR INPUT-SPLIT CONFIGURATIONS IN FUDS CYCLE

Configurati-on	Design Parameters				Normalized Fuel Consumption*	
	$FR$	$R:S$	$P_{MG1\ max}$ (kW)	$P_{MG2\ max}$ (kW)	Initial	Optimized with D.C.
Prius	3.2	2.6	42	60	100.0%	N/A
i1	4.5	2.8	21	42	88.0%	77.0%
i2	5.0	1.6	38	48	101.2%	85.5%
i3	5.0	1.6	42	54	113.4%	110.9%
i4	3.5	3	21	36	82.8%	74.8%
i5	5.0	1.6	42	48	239.5%	146.3%
i6	5.0	1.6	42	30	164.4%	111.1%

\*: The normalized fuel consumption is calculated with battery energy consumption of 0.9 kWh. The fuel consumption results are normalized against that of the Prius for input-split configurations

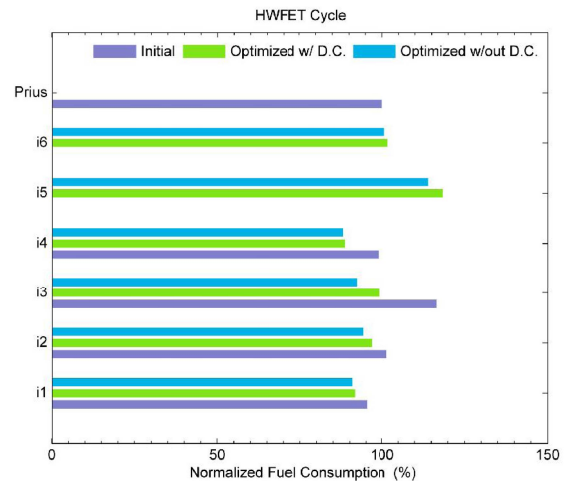


Fig. 13. Normalized fuel consumption results of the initial design and optimized design for the input split on the HWFET cycle.

in Table VI. It is found that configurations i1 and i4 achieve the best fuel economy in the city cycle.

A similar process can be done for the highway fuel economy test (HWFET) cycle and optimized results are shown in Table VII and Fig. 13. Note that for configurations i5 and i6, the initial designs are not feasible to finish the driving cycle. Therefore, only the optimized fuel consumption is shown.

If the target design is to consider both city and highway driving, a weighted average of 55% of city and 45% of highway can be used [20]. The PFC and fuel consumption are calculated by adding the PFC and fuel consumption in FUDS and HWFET together with a scale of 55% and 45%, respectively. Table VIII shows the optimal designs for combined driving condition and their fuel economies. It can be seen that optimal designs using configurations i1 and i4 both achieve good fuel economy.

A further comparison between the best configurations i1 and i4 is established in Table IX. Take the Prius configuration (i1) as an example: the benefits of multiple-mode operations on

TABLE VII  
OPTIMIZED DESIGN PARAMETERS AND FUEL CONSUMPTION FOR  
INPUT-SPLIT CONFIGURATIONS IN THE HWFET CYCLE

Configurati- on	Design Parameters				Normalized Fuel Consumption	
	FR	R:S	$P_{MG1}$ max (kW)	$P_{MG2}$ max (kW)	Initial	Optimized with D.C.
i1	2.0	3.0	29	54	95.3%	91.7%
i2	5.0	1.8	21	60	101.5%	96.7%
i3	4.0	2.0	42	60	116.6%	99.0%
i4	2.0	2.6	21	60	99.1%	88.8%
i5	2.5	1.6	42	60	N/A	118.4%
i6	2.0	1.6	42	54	N/A	101.7%

TABLE VIII  
OPTIMIZED DESIGN PARAMETERS AND FUEL CONSUMPTION FOR  
INPUT-SPLIT CONFIGURATIONS IN COMBINED DRIVING

Configurati- on	Design Parameters				Normalized Fuel Consumption	
	FR	R:S	$P_{MG1}$ max (kW)	$P_{MG2}$ max (kW)	Initial	Optimized with D.C.
i1	3.5	3.0	21	48	93.1%	87.4%
i2	5.0	1.6	38	48	101.5%	94.4%
i3	4.5	2.0	42	60	115.6%	105.3%
i4	3.0	3.0	21	42	94.1%	88.9%
i5	4.0	1.6	42	48	N/A	140.3%
i6	3.0	1.6	42	42	N/A	117.0%

TABLE IX  
NORMALIZED FUEL CONSUMPTION IN COMBINED DRIVING AND  
ACCELERATION PERFORMANCE FOR CONFIGURATIONS i1 AND i4

	Optimized i1		Optimized i4	
	Normalized Fuel consumption	0~60 mph	Normalized Fuel consumption	0~60 mph
All-Modes	87.4%	9.7	88.8%	9.4
Mode 4 only	95.6%	10.4	93.8%	10.6

both fuel economy and launching performance are noticeable. Both optimized designs also use smaller MGs that show potential in reducing cost.

### B. Output-Split Configurations

All six output-split configurations are shown in Fig. 14, where configuration o4 is used in Chevy Volt. For configurations o2 and o3, not only the initial design is infeasible, there is no single feasible design in the entire candidate pool. Either enlarging the MGs size or increase the Final-drive Ratio (FR) will lead to feasible but likely higher cost designs, which means that configurations o2 and o3 are not competitive within the range of vehicle and component sizes we search. Therefore, in Tables X and XI, only configurations o1, o4, o5, and o6 are listed.

As shown in Table XII, good fuel economy can be achieved for combined city and highway driving by configurations o1,

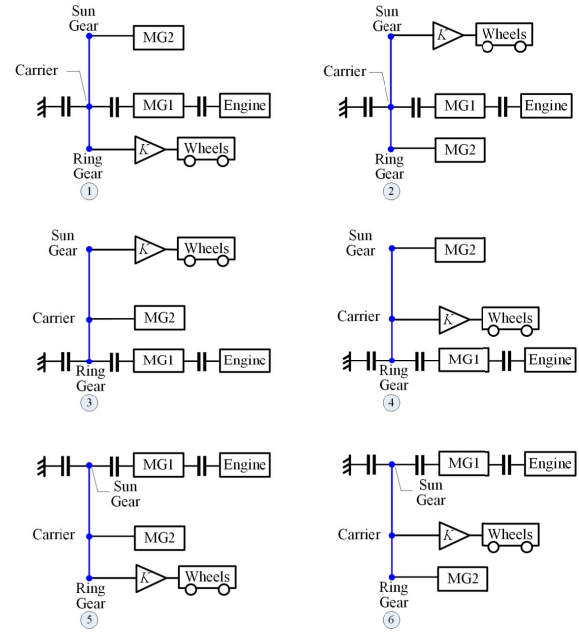


Fig. 14. Six output-split configurations using a single planetary gear.

TABLE X  
OPTIMIZED DESIGN PARAMETERS AND CORRESPONDING  
FUEL CONSUMPTION FOR OUTPUT-SPLIT CONFIGURATIONS  
IN THE FUDS CYCLE

Configurati- on	Design Parameters				Normalized Fuel Consumption*	
	FR	R:S	$P_{MG1}$ max (kW)	$P_{MG2}$ max (kW)	Initial	Optimized
o1	5.0	1.6	49	111	126.3%	98.1%
o4	5.0	1.6	43	56	100.0%	80.4%
o5	5.0	2.6	43	100	N/A	147.4%
o6	5.0	1.6	43	56	148.3%	103.2%

\*: The normalized fuel consumption is calculated with battery energy consumption of 0.9 kWh. The fuel consumption results are normalized against that of the Volt for output-split configurations

TABLE XI  
OPTIMIZED DESIGN PARAMETERS AND CORRESPONDING  
FUEL CONSUMPTION FOR OUTPUT-SPLIT CONFIGURATIONS  
IN THE HWFET CYCLE

Configurati- on	Design Parameters				Normalized Fuel Consumption	
	FR	R:S	$P_{MG1}$ max (kW)	$P_{MG2}$ max (kW)	Initial	Optimized
o1	4.5	1.8	38	111	111.8%	97.7%
o4	2.0	2.6	32	111	100.0%	99.5%
o5	5.0	3.0	54	67	N/A	110.0%
o6	4.5	2.6	54	56	109.5%	105.2%

o4, and o6 compared with the benchmark. Among them, optimized configuration o4 (Volt configuration) has the best fuel economy. Besides o4, o1 has the second best fuel economy after optimization.

TABLE XII  
OPTIMIZED DESIGN PARAMETERS AND CORRESPONDING  
FUEL CONSUMPTION FOR OUTPUT-SPLIT CONFIGURATIONS  
IN COMBINED DRIVING

Configurati- on	Design Parameters				Normalized Fuel Consumption	
	FR	R:S	$P_{MG1}$ max (kW)	$P_{MG2}$ max (kW)	Initial	Optimized
o1	5.0	1.6	43	111	117.0%	99.4%
o4	2.5	2.4	49	111	100.0%	96.6%
o5	5.0	3.0	54	78	N/A	127.1%
o6	4.5	2.4	54	56	123.3%	104.0%

For output-split configurations, the clutches and multiple modes are indispensable. This is because it is inevitable to drag the engine with MG1 in the split mode. In the meantime, the output shaft torque for the split mode is generally lower compared with the input-split configurations. Therefore, the series mode or EV<sub>1</sub> mode is necessary to satisfy the drivability requirement. When the battery SOC level is low, it may not be feasible to drive in the EV<sub>1</sub> mode. In that situation, the availability of the series mode will ensure good launching and driving up hill.

## V. CONCLUSION

A PEARS method for single PG hybrid vehicles is presented in this paper. Comparison with DP results is presented and confirms the validity of the proposed PEARS method. To demonstrate the usefulness of this design method, all 12 configurations of power split hybrid powertrains using a single PG are analyzed and optimal fuel economy designs with respect to variable final drive ratio, R:S ratio and motor sizes are obtained. The optimization results show substantial improvement in fuel economy (which is the design target) and sometimes in drivability (which is a design constraint and not a target). The optimization results also show that it is possible to use smaller electric machines to achieve better fuel economy with guaranteed drivability. Moreover, adding clutches to enable multiple modes also is beneficial compared with single-mode designs.

Among all the input-split configurations, configurations i1 (which Toyota Prius uses) and i4 show similar fuel economy potential. Among all the output-split configurations, configuration o4 (which Chevy Volt uses) shows the best fuel economy potential compared with other configurations. Another configuration (o1) demonstrates comparable fuel economy following if designed properly.

From the design results, it is found that the optimal designs for both input- and output-split configurations proved our intuition: lower FR for city drive while higher FR for high-speed cruising; the optimal designs considering both city and highway driving prefer the FR in between. Meanwhile, we also note that the improvement for configurations i1 and o4 are less significant compared with other configurations since their benchmarks are popular and successful commercialized designs. In addition, the parameters of the optimal design for i4 and o4 are close to the Prius and Volt.

## REFERENCES

- [1] (2010). *Alternative Fuels and Advanced Vehicles Data Center, Data, Analysis, and Trends: Vehicle-HEV Sales by Model* [Online]. Available: <http://www.afdc.energy.gov/afdc/data/vehicles.html>
- [2] B. Conlon, "Comparative analysis of single and combined hybrid electrically variable transmission operating modes," SAE, New York, NY, USA, Tech. Rep. 2005-01-1162, 2005.
- [3] J. Liu and H. Peng, "A systematic design approach for two planetary gear split hybrid vehicles," *Veh. Syst. Dyn.*, vol. 48, no. 11, pp. 1395–1412, Oct. 2010.
- [4] C.-T. Li and H. Peng, "Optimal configuration design for hydraulic split hybrid vehicles," in *Proc. Amer. Control Conf.*, Baltimore, MD, USA, Jun./Jul. 2010, pp. 5812–5817.
- [5] X. Zhang, C.-T. Li, D. Kum, and H. Peng, "Prius<sup>+</sup> and Volt<sup>-</sup>: Configuration analysis of power-split hybrid vehicles with a single planetary gear," *IEEE Trans. Veh. Technol.*, vol. 61, no. 8, pp. 3544–3552, Oct. 2012.
- [6] M. Schmidt, "Two-mode, split power, electro-mechanical transmission," U.S. Patent 5 577 973, Nov. 26, 1996.
- [7] X. Ai and S. Anderson, "Two-mode, compound-split, vehicular transmission having both enhanced speed tractive power," U.S. Patent 6 090 005, Jun. 18, 2000.
- [8] M. Raghavan, N. Bucknor, and J. Hendrickson, "Electrically variable transmission having three interconnected planetary gear sets, two clutches and two brakes," U.S. Patent 7 179 187 Feb. 24, 2007.
- [9] D. Hermance, "Toyota hybrid system," in *Proc. SAE TOPTTEC Conf.*, Albany, NY, USA, 1999.
- [10] N. Jalil, N. Kheir, and M. Salman, "A rule-based energy management strategy for a series hybrid vehicle," in *Proc. Amer. Control Conf.*, Albuquerque, NM, USA, vol. 1. Jun. 1997, pp. 689–693.
- [11] G. Pagalelli, S. Delprat, T. M. Guerra, J. Rimaux, and J. J. Santin, "Equivalent consumption minimization strategy for parallel hybrid powertrains," in *Proc. IEEE 55th Veh. Technol. Conf.*, vol. 4, 2002, pp. 2076–2081.
- [12] A. Sciarretta, M. Back, and L. Guzzella, "Optimal control of parallel hybrid electric vehicles," *IEEE Trans. Veh. Technol.*, vol. 12, no. 3, pp. 352–363, May 2004.
- [13] S. Delprat, J. Lauber, T. M. Guerra, and J. Rimaux, "Control of a parallel hybrid powertrain: Optimal control," *IEEE Trans. Veh. Technol.*, vol. 53, no. 3, pp. 872–881, May 2004.
- [14] S. Delprat, T. M. Guerra, and J. Rimaux, "Control strategies for hybrid vehicles: Optimal control," in *Proc. 56th IEEE Veh. Technol. Conf.*, May. 2002, pp. 1681–1685.
- [15] N. Kim, S. Cha, and H. Peng, "Optimal control of hybrid electric vehicles based on Pontryagin's minimum principle," *IEEE Trans. Control Syst. Technol.*, vol. 19, no. 5, pp. 1279–1287, Aug. 2010.
- [16] C.-C. Lin, H. Peng, J. Grizzle, and J.-M. Kang, "Power management strategy for a parallel hybrid electric truck," *IEEE Trans. Control Syst. Technol.*, vol. 11, no. 6, pp. 839–849, Nov. 2003.
- [17] J. Liu and H. Peng, "Control optimization for a power-split hybrid vehicle," in *Proc. Amer. Control Conf.*, Jun. 2006, pp. 466–471.
- [18] H. Benford and M. Leising, "The lever analogy: A new tool in transmission analysis," SAE, New York, NY, USA, Tech. Rep. 810102, 1981.
- [19] X. Zhang, C. Li, D. Kum, H. Peng, and J. Sun, "Configuration analysis for power split hybrid vehicles with multiple operating modes," in *Proc. AVEC Conf.*, Seoul, Korea, 2012.
- [20] (2013, May 20). *Gasoline Vehicles: Learn More About the New Label*. [Online]. Available: <http://www.fueleconomy.gov/feg/label/learn-more-gasoline-label.shtml>



**Xiaowu Zhang** received B.S. and M.S. degrees in mechanical engineering from Beihang University, Beijing, China, and the University of Michigan, Ann Arbor, MI, USA, in 2010 and 2012, respectively, where he is currently pursuing the Ph.D. degree in mechanical engineering.

His current research interests include optimal control, sizing and design of clean energy systems, and configuration design and control of split hybrid vehicles.



**Hwei Peng** received the Ph.D. degree in mechanical engineering from the University of California at Berkeley, Berkeley, CA, USA, in 1992.

He is currently a Professor with the Department of Mechanical Engineering, University of Michigan, Ann Arbor, MI, USA. His current research interests include adaptive control and optimal control, with emphasis on their applications to vehicular and transportation systems, design and control of electrified vehicles, and connected/automated vehicles.

Dr. Peng is a fellow of the Society of Automotive Engineers and the American Society of Mechanical Engineers. He is a ChangJiang Scholar with the Tsinghua University, Beijing, China.



**Jing Sun** (F'04) received the B.S. and M.S. degrees from the University of Science and Technology of China, Hefei, China, in 1982 and 1984 respectively, and the Ph.D. degree from the University of Southern California, Los Angeles, CA, USA, in 1989.

She was an Assistant Professor with the Department of Electrical and Computer Engineering, Wayne State University, Detroit, MI, USA, from 1989 to 1993. She joined the Ford Research Laboratory, the Department of Powertrain Control Systems, Dearborn, MI, USA, in 1993. She joined the faculty

of the College of Engineering with the University of Michigan, Ann Arbor, MI, USA, in 2003, where she is currently a Professor with the Department of Naval Architecture and Marine Engineering and the Department of Electrical Engineering and Computer Science. She holds 37 U.S. patents, and has co-authored a textbook on robust adaptive control. Her current research interests include system and control theory, and its applications to marine and automotive propulsion systems.

Dr. Sun is one of the three recipients of the 2003 IEEE Control System Technology Award.